

ORIGINAL ARTICLE

OPEN

The BHVI-EyeMapper: Peripheral Refraction and Aberration Profiles

Cathleen Fedtke*, Klaus Ehrmann[†], Darrin Falk, Ravi C. Bakaraju[‡], and Brien A. Holden*

ABSTRACT

Purpose. The aim of this article was to present the optical design of a new instrument (BHVI-EyeMapper, EM), which is dedicated to rapid peripheral wavefront measurements across the visual field for distance and near, and to compare the peripheral refraction and higher-order aberration profiles obtained in myopic eyes with and without accommodation.

Methods. Central and peripheral refractive errors (M , J_{180} , and J_{45}) and higher-order aberrations ($C[3, 1]$, $C[3, 3]$, and $C[4, 0]$) were measured in 26 myopic participants (mean [\pm SD] age, 20.9 [\pm 2.0] years; mean [\pm SD] spherical equivalent, -3.00 [\pm 0.90] diopters [D]) corrected for distance. Measurements were performed along the horizontal visual field with (-2.00 to -5.00 D) and without ($+1.00$ D fogging) accommodation. Changes as a function of accommodation were compared using tilt and curvature coefficients of peripheral refraction and aberration profiles.

Results. As accommodation increased, the relative peripheral refraction profiles of M and J_{180} became significantly ($p < 0.05$) more negative and the profile of M became significantly ($p < 0.05$) more asymmetric. No significant differences were found for the J_{45} profiles ($p > 0.05$). The peripheral aberration profiles of $C[3, 1]$, $C[3, 3]$, and $C[4, 0]$ became significantly ($p < 0.05$) less asymmetric as accommodation increased, but no differences were found in the curvature.

Conclusions. The current study showed that significant changes in peripheral refraction and higher-order aberration profiles occurred during accommodation in myopic eyes. With its extended measurement capabilities, that is, permitting rapid peripheral refraction and higher-order aberration measurements up to visual field angles of ± 50 degrees for distance and near (up to -5.00 D), the EM is a new advanced instrument that may provide additional insights in the ongoing quest to understand and monitor myopia development.

(Optom Vis Sci 2014;91:1199–1207)

Key Words: peripheral refraction, aberrations, instrumentation, myopia, accommodation

Myopia is thought to be of multifactorial etiology, caused by an interaction between environmental and genetic factors. In recent years, optical factors, such as relative peripheral hyperopic defocus^{1–3} and the greater accommodative lag^{4,5} found in myopic eyes, have been linked to axial growth of the eye and, thus, myopia development. Currently available techniques for the measurement of peripheral refraction and accommodative responses are limited, making the investigation of such factors difficult. Specifically, measurement of the peripheral optics

of the eye with commercial instruments is cumbersome as it requires modification of the instrument and/or the measurement technique.⁶ Such modifications can be traced back as far as 1931, when Ferree et al.⁷ attempted to measure peripheral refraction using a manual optometer. Since then, many other refraction techniques have been used, including subjective refraction,^{8,9} streak retinoscopy,^{10,11} double-pass technique,^{12,13} and more current techniques, such as photorefractometry,^{14,15} autorefractometry,^{16,17} and aberrometry.^{18–20} One of the commercial instruments most frequently used for peripheral refraction measurements is the Shin-Nippon autorefractor,⁶ which has the advantage that it is an objective instrument and thus easy to use and because of its open-view design, its use for peripheral measurements requires the fewest modifications when compared with that of closed-view instruments. When adopted for peripheral refraction measurements, all of these instruments require some form of off-axis fixation or instrument rotation, as well as independent instrument realignments per measurement angle and repeat. This not only results in a prolonged measurement procedure but also can lead to

*PhD, FAAO

[†]PhD

[‡]BOptom, PhD, FAAO

The Brien Holden Vision Institute, Sydney, New South Wales, Australia (all authors); The Vision Cooperative Research Centre, Sydney, New South Wales, Australia (CF, BAH); and School of Optometry and Vision Science, The University of New South Wales, Sydney, New South Wales, Australia (KE, BAH).

This is an open-access article distributed under the terms of the Creative Commons Attribution-NonCommercial-NoDerivatives 3.0 License, where it is permissible to download and share the work provided it is properly cited. The work cannot be changed in any way or used commercially.

potential measurement errors.²¹ In recent years, the need for faster instruments requiring no off-axis fixation, instrument rotation, or numerous realignments across one meridian has been recognized, and first research prototypes, such as the eccentric scanning photoretinoscope of Taberero and Schaeffel,²² the scanning Hartmann-Shack aberrometers of Jaeken and Artal²³ and of Wei and Thibos,²⁴ and the BHVI-EyeMapper (EM),²⁵ have been introduced. One major advantage of these new instruments is the speed in measuring peripheral refraction when compared with that of the modified techniques. Furthermore, the instruments based on the Hartmann-Shack principle have the added advantage of being able to assess both refractive errors and higher-order ocular aberrations across the visual field.

A number of studies have previously assessed the peripheral optics of the eye during near viewing, which showed no or small changes as a function of accommodation.^{17,26–30} To further assess the potential relationship between relative peripheral hyperopic defocus and accommodative lag with respect to myopia development, instruments that can measure the peripheral optics of the eye as well as accommodative responses can be of particular use. Whereas the Scanning PhotoRefractor and the Scanning Hartmann-Shack Wavefront Sensor are able to present a near target via their instruments' open-view design, the EM permits accommodative response measurements via its internal moving fixation target.

This article aims to present the optical design of an aberrometer, the EM, and the application of this new instrument to compare the horizontal peripheral refractive error and higher-order aberration profiles of myopic eyes for measurements performed at different accommodative demands. Results are compared with data obtained with other peripheral refraction techniques.

METHODS

Instrumentation

The EM (Fig. 1) is a research instrument developed at the Brien Holden Vision Institute, Sydney, Australia, dedicated to the measurement of the global wavefront of the eye, that is, central and peripheral wavefront along several visual field meridians. The instrument consists of five optical paths: the illumination path, the reflection path, the fixation path, the pupil imaging path, and the deflection system (Fig. 2), which were designed using the optical design software ZEMAX EE (Zemax Development Corporation, Washington, USA). The deflection system is the most distinctive feature of the EM, permitting a rapid visual field scan. It comprises an intricate arrangement of 33 stationary mirrors and 1 scanning mirror (Cambridge Technology, Cambridge, USA; Model 6240H), which together permit 11 wavefront measurements from -50 to $+50$ degrees in 10-degree steps in less than half a second. The particular arrangement of mirrors provides equal optical path lengths for all 11 scanning positions, achieved by deflecting the beam upward, out of the scanning plane and back, by mirrors positioned at different heights (Fig. 3). Mirror heights for the peripheral angles are successively reduced to compensate for the longer optical path distances in the scanning plane. Mirror pairs M1 and M3, as well as lens pairs L1 ($f' = 100$ mm) and L2 ($f' = 100$ mm), are arranged symmetrically with respect to the vertical mirror plane of M2. In combination with this particular arrangement of the 33



FIGURE 1.

Front view of the EM instrument. A color version of this figure is available online at www.optvissci.com.

mirrors in the deflection system, the 11 relay lens pairs ensure that the center of the eye's pupil is conjugate with the pivot of the scanning mirror and that equal magnification and defocus are maintained for the consistent capture, analysis, and comparability of the wavefront for each of the 11 scan angles. The second relay lens pair (L3-L4, $f' = 100$ and 50 mm) with a magnification factor of 0.5 was used to capture the eye's wavefront errors at the plane conjugate to the pivot of the scanning mirror by use of a Hartmann-Shack sensor (HASO—32 eye, Imagine Eyes, France). This sensor features high resolution and a wide dynamic range, with 1280 sub-apertures located in a monolithic 40 by 32 microlens array.

The instrument's baseplate can be rotated from 0 to 90 degrees in 15-degree steps via bearing assemblies and two curved rails that permit measurements of horizontal, vertical, and five oblique (i.e., 15, 30, 45, 60, and 75 degrees) visual field meridians. In addition to permitting global wavefront measurements, the deflection system is also used for the alignment of the pupil. The equal optical path lengths of the deflection system permit focused imaging of the pupil from different observation angles for improved lateral and axial pupil alignment, facilitating more consistent measurements.

As for the fixation path, the EM is equipped with a back-illuminated fixation target mounted on a motorized translation stage (M+122.2DD, Physik Instrumente GmbH & Co KG, Germany) to facilitate accommodative response measurements (Fig. 2). The software adjustable linear stage is positioned on a continuous scale to create a range of object vergences from $+1.00$

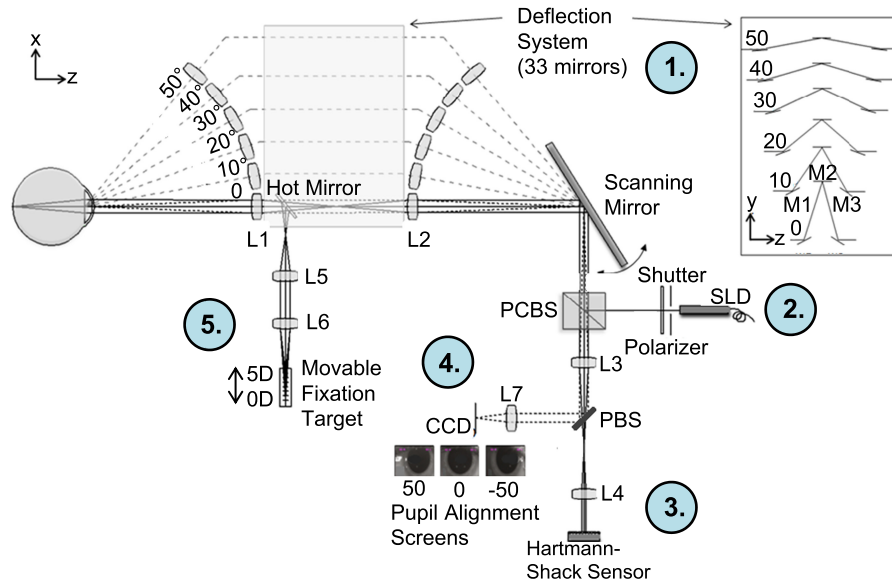


FIGURE 2.

Layout of the EM instrument design (1. deflection system, 2. illumination path, 3. reflection path, 4. pupil imaging path, and 5. fixation path). For clarity, only the central path and 5 of the 10 peripheral paths are shown. A color version of this figure is available online at www.optvissci.com.

diopter (D) (fogging) to -5.00 D (accommodative demand), with the target being telecentric in object space.

The instrument uses a near-infrared superluminescent diode with a wavelength of 830 nm. Light exposure to the eye is controlled via a mechanical shutter and is below the maximum permissible exposure limit (i.e., below 1.03 mW for a single spot exposure duration of 45 milliseconds) as defined by the ANSI Z136.1-2007 Standards.³¹

The EM has previously been validated for distance²⁵ and near³² measurements against a commercially available aberrometer, the COAS-HD (Complete Ophthalmic Analysis System), and an open-view autorefractor, the Shin-Nippon NVision K5001. The main findings of these studies were that the relative peripheral refraction profiles were in good agreement between the instruments, the lowest measurement variability was obtained with the EM, and on-axis measurements obtained with the two closed-view

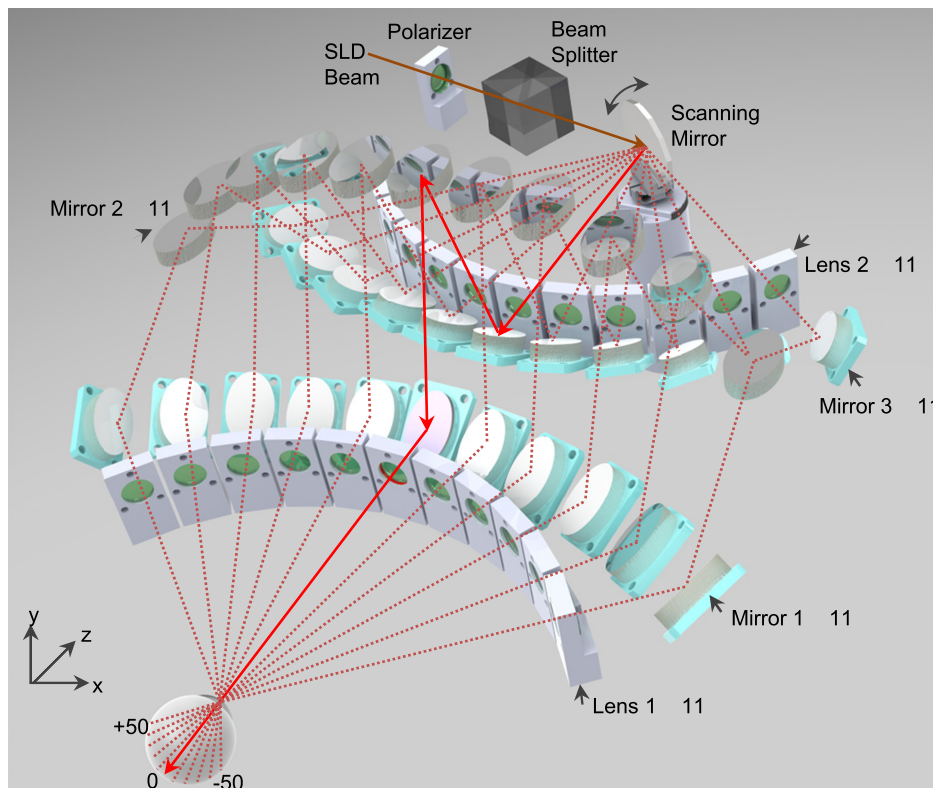


FIGURE 3.

Three-dimensional layout of the deflection system. A color version of this figure is available online at www.optvissci.com.

instruments, that is, the COAS and the EM, showed some impact of instrument myopia.

Participants

Measurements were performed on a total of 26 experienced myopic contact lens wearers, dispensed with single-vision AIR OPTIX AQUA lenses (lotrafilcon B, CIBA VISION, USA), which have minimal spherical aberration³³ and consequently a small impact on peripheral measurements. Participants were corrected for best distance vision, which ensured that the same accommodative effort was achieved when the fixation target was viewed at near. Participants were aged between 18 and 25 years and with a myopic contact lens prescription between -1.00 and -4.00 D, astigmatism not greater than 1.00 D, and anisometropia between the two eyes of 1.00 D or less.

Measurements were performed in the right eyes along the horizontal visual field meridian at five demand settings ($+1.00$, -2.00 , -3.00 , -4.00 , and -5.00 D). Five independent repeats were performed at each demand setting. Participants were asked to view the fixation target—a “6/12” equivalent reduced Snellen letter E—and to keep it clear in focus during the measurements. The left eye was occluded. The protocol and informed consent were reviewed and approved by an independent ethics committee and the research followed the tenets of the Declaration of Helsinki. The study was registered with the Australian and New Zealand Clinical Trial Registry (ACTRN12611001004954) before the enrolment of participants.

Analysis

To permit the comparison of different peripheral visual field angles, the wavefront was analyzed over a circular 4-mm aperture at all eccentricities. Absolute central and peripheral refractive errors and higher-order aberrations were summarized as means \pm SD at specific angles of eccentricity. Refraction data were calculated from wavefront aberrations and quantified using the three refractive power vectors: M (spherical equivalent), J_{180} (with/against-the-rule astigmatism), and J_{45} (oblique astigmatism). Analysis was performed for the aberration coefficients $C[3, 1]$, $C[3, 3]$, and $C[4, 0]$. Other terms were not reported because of relatively small changes across the visual field. For comparison of the peripheral refraction and higher-order aberration profiles between the different accommodative states, tilt and curvature coefficients of the relative peripheral refraction and aberration

TABLE 1.

Mean on-axis refraction (in diopters) as measured with the EM at each accommodative demand setting

| Accommodative demand | M | | J_{180} | | J_{45} | |
|----------------------|-------|----------|-----------|----------|----------|----------|
| | Mean | \pm SD | Mean | \pm SD | Mean | \pm SD |
| +1.00 D | -0.61 | 0.35 | 0.05 | 0.19 | -0.02 | 0.14 |
| -2.00 D | -1.88 | 0.33 | 0.07 | 0.23 | 0.00 | 0.15 |
| -3.00 D | -2.73 | 0.38 | 0.08 | 0.25 | 0.00 | 0.18 |
| -4.00 D | -3.57 | 0.52 | 0.09 | 0.25 | 0.00 | 0.18 |
| -5.00 D | -4.34 | 0.72 | 0.12 | 0.24 | 0.00 | 0.19 |

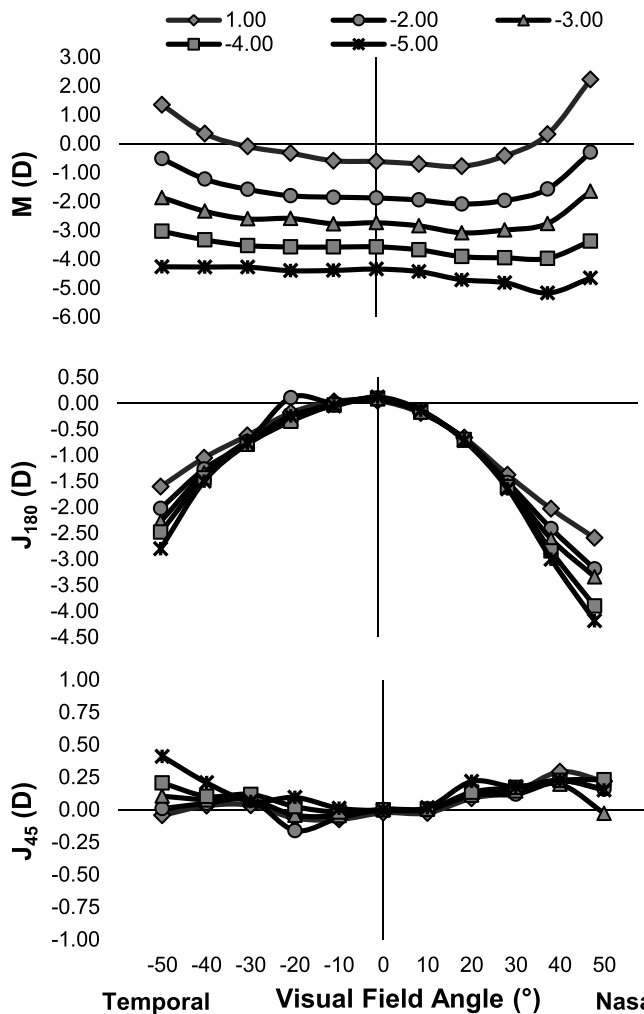


FIGURE 4.

Peripheral refraction profiles for M , J_{180} , and J_{45} as measured at different demand settings.

profiles were estimated by fitting a second-order polynomial (least squares regression) for each refractive power vector and each aberration term. The dependent variables were the refractive power vectors and the aberration terms, and the independent variables (covariates) were visual field angle and the quadratic term of visual field angle. The estimated tilt and curvature coefficients were summarized as means \pm SD across accommodative states. Whereas tilt coefficients were used to compare the symmetry of the profiles, the curvature coefficients were used to compare the curvature of the profiles. Relative to on-axis, a positive tilt coefficient indicates a positive measurement in the nasal visual field and a negative measurement in the temporal visual field. The opposite applies for a negative tilt coefficient. A positive curvature coefficient indicates a positive measurement in both visual fields and *vice versa* for a negative curvature coefficient. The estimated tilt and curvature coefficients were compared between accommodative states using univariate linear mixed models. Outcome variables for linear mixed models were the estimated tilt and curvature coefficients of the refractive power vectors and the aberration terms. Accommodative state was modeled as repeated fixed factor (independent variable) with participant ID included for random intercepts. *Post hoc* multiple comparisons were corrected using

Bonferroni correction. Level of statistical significance was set at 5%. Analysis was performed using SPSS 21 (IBM, New York, USA).

RESULTS

Of the 26 participants, 73.1% were female; the mean (\pm SD) age was 20.9 (\pm 2.0) years; and the mean (\pm SD) spherical equivalent was -3.00 (\pm 0.90) D. Table 1 shows the mean on-axis refraction for M , J_{180} , and J_{45} as measured at each accommodative demand setting. Measurements performed at near showed an increase in accommodative lag with increase in accommodation. Specifically, the slope for the accommodative response function as measured between -2.00 and -5.00 D was significantly less negative (slope = -0.821 , $p < 0.05$) when compared with the ideal slope of $+1.00$. Distance measurements were -0.61 ± 0.35 D, which, as reported previously,²⁵ can be attributed to the effect of instrument myopia caused by the closed-view design of the EM. On-axis J_{180} increased slightly but significantly as a function of accommodation (slope = 0.016 , $p = 0.015$). No significant change was found for J_{45} (slope = -0.002 , $p = 0.721$).

Fig. 4 shows the peripheral refraction profiles for M , J_{180} , and J_{45} as a function of accommodation, and Table 2 shows the

corresponding tilt and curvature coefficients for the profiles with significant changes during accommodation. Relative to on-axis, the curvature of the M profile changed significantly from being relatively hyperopic in the periphery for distance measurements to being relatively myopic at an accommodative demand of -5.00 D (curvature $_{+1.00\text{ D}} = 0.0006$, curvature $_{-5.00\text{ D}} = -0.0002$, $p < 0.05$). The greatest relative M difference of 2.91 D was found between measurements performed at distance ($+1.00$ D) and near (-5.00 D) at the 50-degree nasal visual field angle. Moreover, as accommodation increased, the nasal-temporal asymmetry of the M profiles also increased, which was significant between distance ($+1.00$ D) and -4.00 D near measurements (Table 2, tilt $_{+1.00\text{ D}} = -0.0032$, tilt $_{-4.00\text{ D}} = -0.0078$, $p = 0.037$) as well as between distance and -5.00 D near measurements (Table 2, tilt $_{+1.00\text{ D}} = -0.0032$, tilt $_{-5.00\text{ D}} = -0.0090$, $p = 0.002$). As for the J_{180} profiles, there was no significant difference ($p = 0.113$) in the asymmetry as a function of accommodation with tilt coefficients ranging from -0.0124 to -0.0159 at accommodative demand settings of $+1.00$ and -5.00 D, respectively. However, the curvature of the J_{180} profile became significantly more negative (e.g., curvature $_{+1.00\text{ D}} = -0.0010$, curvature $_{-5.00\text{ D}} = -0.0014$) as accommodation increased ($p < 0.05$). Again, the greatest relative

TABLE 2.

Comparison of the tilt and curvature coefficients for the peripheral refraction profiles of M , J_{180} , and J_{45} with changing accommodation

| Variables | Accommodative demand | Mean | SD | p | Post hoc analysis | | | | | |
|--------------------|----------------------|---------|---------|--------|-------------------|---------|---------|---------|---------|-------|
| | | | | | +1.00 D | -2.00 D | -3.00 D | -4.00 D | -5.00 D | |
| Relative M | +1.00 D | -0.0032 | 0.0162 | | — | 1.000 | 0.504 | 0.037 | 0.002 | |
| | -2.00 D | -0.0053 | 0.0151 | | 1.000 | — | 1.000 | 1.000 | 0.174 | |
| | Tilt | -3.00 D | -0.0063 | 0.0145 | 0.003 | 0.504 | 1.000 | — | 1.000 | 0.849 |
| | | -4.00 D | -0.0078 | 0.0152 | | 0.037 | 1.000 | 1.000 | — | 1.000 |
| | | -5.00 D | -0.0090 | 0.0163 | | 0.002 | 0.174 | 0.849 | 1.000 | — |
| | | +1.00 D | 0.0006 | 0.0007 | | — | 0.000 | 0.000 | 0.000 | 0.000 |
| | | -2.00 D | 0.0003 | 0.0007 | | 0.000 | — | 0.048 | 0.000 | 0.000 |
| | Curvature | -3.00 D | 0.0002 | 0.0007 | 0.000 | 0.000 | 0.048 | — | 0.082 | 0.000 |
| | | -4.00 D | 0.0000 | 0.0007 | | 0.000 | 0.000 | 0.082 | — | 0.051 |
| | | -5.00 D | -0.0002 | 0.0007 | | 0.000 | 0.000 | 0.000 | 0.051 | — |
| +1.00 D | | -0.0010 | 0.0003 | | | 0.000 | 0.000 | 0.000 | 0.000 | |
| Relative J_{180} | +1.00 D | -0.0124 | 0.0085 | | | | | | | |
| | -2.00 D | -0.0146 | 0.0098 | | | | | | | |
| | Tilt | -3.00 D | -0.0146 | 0.0091 | 0.113 | | | | | |
| | | -4.00 D | -0.0149 | 0.0091 | | | | | | |
| | | -5.00 D | -0.0159 | 0.0102 | | | | | | |
| | | +1.00 D | -0.0010 | 0.0003 | | | 0.000 | 0.000 | 0.000 | 0.000 |
| | | -2.00 D | -0.0012 | 0.0003 | | 0.000 | | 1.000 | 0.004 | 0.000 |
| | Curvature | -3.00 D | -0.0013 | 0.0003 | 0.000 | 0.000 | 1.000 | | 0.299 | 0.003 |
| | | -4.00 D | -0.0014 | 0.0003 | | 0.000 | 0.004 | 0.299 | | 1.000 |
| | | -5.00 D | -0.0014 | 0.0004 | | 0.000 | 0.000 | 0.003 | 1.000 | |
| +1.00 D | | 0.0027 | 0.0082 | | | | | | | |
| Relative J_{45} | +1.00 D | 0.0027 | 0.0082 | | | | | | | |
| | -2.00 D | 0.0023 | 0.0083 | | | | | | | |
| | Tilt | -3.00 D | 0.0017 | 0.0080 | 0.418 | | | | | |
| | | -4.00 D | 0.0016 | 0.0088 | | | | | | |
| | | -5.00 D | 0.0011 | 0.0092 | | | | | | |
| | | +1.00 D | 0.0001 | 0.0001 | | | | | | |
| | | -2.00 D | 0.0001 | 0.0001 | | | | | | |
| | Curvature | -3.00 D | 0.0001 | 0.0001 | 0.615 | | | | | |
| | | -4.00 D | 0.0001 | 0.0001 | | | | | | |
| | | -5.00 D | 0.0001 | 0.0002 | | | | | | |

difference was found between measurements performed at distance (+1.00 D) and near (−5.00 D) at the 50-degree nasal visual field angle, which was as great as 1.68 D. No significant differences were found in the curvatures ($p = 0.615$) and symmetries ($p = 0.418$) of the peripheral refraction profiles of J_{45} as a function of accommodation.

Table 3 shows the mean on-axis aberrations for $C[3, 1]$, $C[3, 3]$, and $C[4, 0]$ as measured at each accommodative demand. With the exception of $C[4, 0]$ between −2.00 and −3.00 D, all coefficients became smaller with increasing accommodation, but this decrease was only significant for $C[3, 3]$ ($p = 0.012$).

Fig. 5 shows the peripheral aberration profiles of $C[3, 1]$, $C[3, 3]$, and $C[4, 0]$ as a function of accommodation. Relative to on-axis, the $C[3, 1]$ and $C[3, 3]$ measures increased with increasing visual field angle in the temporal visual field and decreased in the nasal visual field. This nasal-temporal asymmetry (i.e., the negative tilt) seen in the profiles decreased significantly as accommodation increased (Table 4, $p < 0.05$). For example, at the 50-degree nasal visual field angle, the differences in $C[3, 1]$ and $C[3, 3]$ between distance (+1.00 D) and near (−5.00 D) measurements were 0.10 and 0.12 μm , respectively.

Regardless of accommodative demand, the relative peripheral aberration profile of $C[4, 0]$ became increasingly more negative up to visual field angles of +30 and −40 degrees. As accommodation increased, no significant differences were found with respect to the curvature of the profiles ($p > 0.05$); however, the asymmetry of the profiles decreased significantly between distance (+1.00 D) and −5.00 D near measurements (Table 4, $\text{tilt}_{+1.00\text{ D}} = 0.0009$, $\text{tilt}_{-5.00\text{ D}} = 0.0001$, $p < 0.05$).

DISCUSSION

Peripheral Refraction Techniques

Although myopia is associated with peripheral hyperopia,¹⁻³ it is yet to be confirmed that peripheral hyperopia is present before myopia first develops and that it is the cause for axial growth. In the last few years, the association between peripheral hyperopia and myopia has led to an increased interest in the measurement of peripheral refraction.⁶ Most commonly, commercially available instruments have been adopted for this purpose, requiring modification to the instrument setup and alignment procedure. Besides the inconvenience with respect to the realignment requirements, there is some indication that eye turn can affect peripheral refraction measurements^{7,14} possibly attributed to pressure of the external muscles leading to a temporary elongation of the eye during prolonged peripheral fixation. However, that remains inconclusive as

TABLE 3.

Mean on-axis aberrations (in micrometers) as measured with the EM at each accommodative demand setting

| Accommodative demand | $C[3, 1]$ | | $C[3, 3]$ | | $C[4, 0]$ | |
|----------------------|-----------|-------|-----------|-------|-----------|-------|
| | Mean | SD | Mean | SD | Mean | SD |
| +1.00 D | 0.061 | 0.141 | 0.044 | 0.106 | −0.022 | 0.123 |
| −2.00 D | 0.044 | 0.107 | 0.024 | 0.082 | −0.068 | 0.133 |
| −3.00 D | 0.039 | 0.098 | 0.015 | 0.048 | −0.070 | 0.118 |
| −4.00 D | 0.036 | 0.076 | 0.008 | 0.041 | −0.087 | 0.114 |
| −5.00 D | 0.026 | 0.065 | 0.004 | 0.043 | −0.081 | 0.108 |

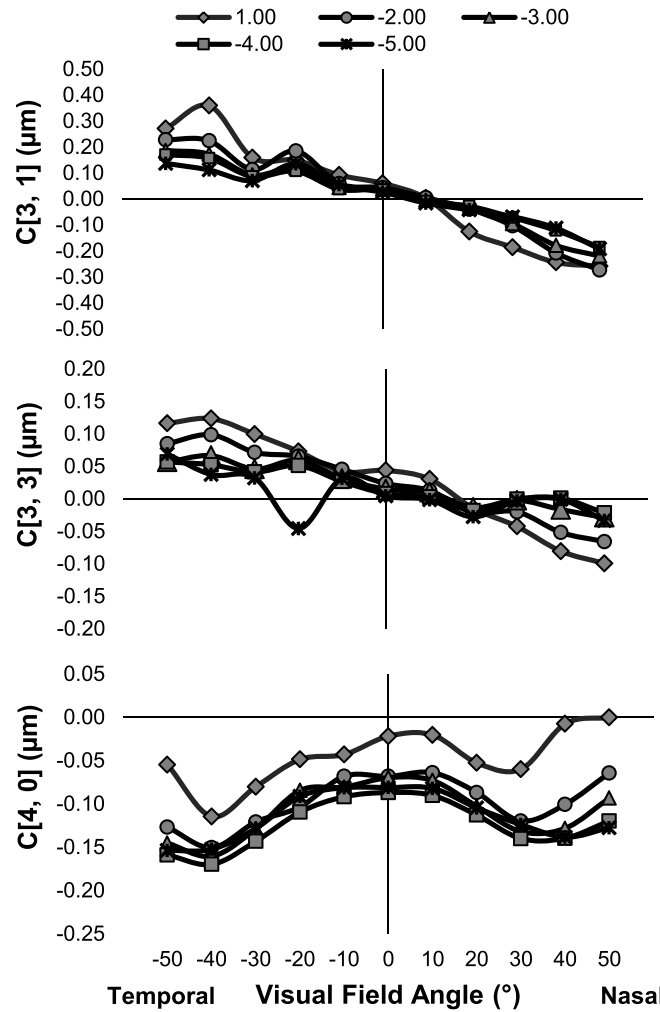


FIGURE 5. Peripheral aberration profiles for $C[3, 1]$, $C[3, 3]$, and $C[4, 0]$ as measured at different demand settings.

a study by Radhakrishnan and Charman³⁴ failed to confirm the difference in refraction between eye and head turn.

Over the last few years, several research instruments that are dedicated to the measurement of peripheral refraction^{22-24,35} and that permit visual field scanning without the need for head or eye turn have been developed. All the instruments differ somewhat in their operation principles and features. For example, the scanning photorefractor of Taberero and Schaeffel²² permits continuous refraction readings (limited to spherical errors) within about 4 seconds across the horizontal visual field via a rotational and translational hot mirror. The scanning Shack-Hartmann aberrometer by Wei and Thibos²⁴ uses custom-designed, three-element, double-pass scanning lenses and two scanning mirrors to perform the visual field scan. By use of these lenses, the instrument permits measurements within 7 to 8 seconds ranging from −15 to +15 degrees in 5-degree steps along six visual field meridians. Like the scanning photorefractor of Taberero and Schaeffel, the open-view scanning wavefront sensor of Jaeken and Artal²³ measures refraction continuously within 2 seconds across the horizontal visual field. This instrument has a high-speed Hartmann-Shack detector mounted on a rotating arm that pivots around the center of the measured eye. A cold mirror provides

TABLE 4.

Comparison of the tilt and curvature coefficients for the peripheral aberration profiles of C[3, 1], C[3, 3], and C[4, 0] with changing accommodation

| Variables | Accommodative demand | Mean | SD | p | Post hoc analysis | | | | | |
|------------------|----------------------|---------|---------|--------|-------------------|---------|---------|---------|---------|-------|
| | | | | | +1.00 D | -2.00 D | -3.00 D | -4.00 D | -5.00 D | |
| Relative C[3, 1] | +1.00 D | -0.0068 | 0.0097 | | — | 0.128 | 0.003 | 0.000 | 0.000 | |
| | -2.00 D | -0.0048 | 0.0081 | | 0.128 | — | 1.000 | 0.442 | 0.236 | |
| | Tilt | -3.00 D | -0.0039 | 0.0071 | 0.000 | 0.003 | 1.000 | — | 1.000 | 1.000 |
| | -4.00 D | -0.0032 | 0.0063 | | 0.000 | 0.442 | 1.000 | — | 1.000 | |
| | -5.00 D | -0.0030 | 0.0058 | | 0.000 | 0.236 | 1.000 | 1.000 | — | |
| | Curvature | +1.00 D | 0.0000 | 0.0002 | | | | | | |
| | -2.00 D | 0.0000 | 0.0001 | | | | | | | |
| | -3.00 D | 0.0000 | 0.0001 | 0.394 | | | | | | |
| | -4.00 D | 0.0000 | 0.0001 | | | | | | | |
| | -5.00 D | 0.0000 | 0.0001 | | | | | | | |
| Relative C[3, 3] | +1.00 D | -0.0024 | 0.0032 | | — | 1.000 | 0.008 | 0.001 | 0.000 | |
| | -2.00 D | -0.0018 | 0.0031 | | 1.000 | — | 0.556 | 0.121 | 0.002 | |
| | Tilt | -3.00 D | -0.0011 | 0.0031 | 0.000 | 0.008 | 0.556 | — | 1.000 | 0.752 |
| | -4.00 D | -0.0008 | 0.0028 | | 0.001 | 0.121 | 1.000 | — | 1.000 | |
| | -5.00 D | -0.0003 | 0.0028 | | 0.000 | 0.002 | 0.752 | 1.000 | — | |
| | Curvature | +1.00 D | 0.0000 | 0.0001 | | | | | | |
| | -2.00 D | 0.0000 | 0.0001 | | | | | | | |
| | -3.00 D | 0.0000 | 0.0000 | 0.389 | | | | | | |
| | -4.00 D | 0.0000 | 0.0000 | | | | | | | |
| | -5.00 D | 0.0000 | 0.0001 | | | | | | | |
| Relative C[4, 0] | +1.00 D | 0.0009 | 0.0017 | | — | 0.765 | 0.054 | 0.075 | 0.015 | |
| | -2.00 D | 0.0004 | 0.0014 | | 0.765 | — | 1.000 | 1.000 | 1.000 | |
| | Tilt | -3.00 D | 0.0002 | 0.0008 | 0.012 | 0.054 | 1.000 | — | 1.000 | 1.000 |
| | -4.00 D | 0.0002 | 0.0008 | | 0.075 | 1.000 | 1.000 | — | 1.000 | |
| | -5.00 D | 0.0001 | 0.0009 | | 0.015 | 1.000 | 1.000 | 1.000 | — | |
| | Curvature | +1.00 D | 0.0000 | 0.0001 | | | | | | |
| | -2.00 D | 0.0000 | 0.0001 | | | | | | | |
| | -3.00 D | 0.0000 | 0.0001 | 0.347 | | | | | | |
| | -4.00 D | 0.0000 | 0.0001 | | | | | | | |
| | -5.00 D | 0.0000 | 0.0000 | | | | | | | |

open-field viewing for the participants. As with the EM, one design goal of this wavefront sensing technique was to maintain equal path lengths at each measuring angle.

Unlike the scanning aberrometer by Wei and Thibos, in which all peripheral measurements are performed via the same double-pass scanning lenses, the deflection system of the EM has individual paths for each peripheral measurement angle and thus permits measurements up to ± 50 degrees. Distinct from the instruments by Taberner and Schaeffel and Jaeken and Artal that require some large, externally moving elements to perform a continuous peripheral refraction scan for the assessment of a complete peripheral refraction profile, the EM's deflection system comprises 11 individual measurement paths to perform a visual field scan within less than 1 second, which minimizes the impact of fluctuating accommodation and/or fluctuating fixation on the refraction measurements. A further feature of this instrument is the fully automated data acquisition, processing, and analysis to provide results in real time for immediate evaluation and subsequent archiving.

With the exception of the scanning Shack-Hartmann aberrometer by Wei and Thibos, all other instruments/setups can measure accommodative responses, either via the open-view design (Scanning PhotoRefractor and Scanning Hartmann-Shack Wavefront

Sensor) or via an internal movable fixation target positioned telecentric in object space (EM).

When comparing the features of these peripheral refraction instruments, it is evident that each instrument possesses advantages and disadvantages and it is anticipated that further refinements will follow. Ultimately, such instruments have the potential to be used not only for research but also in general clinical practice as myopia monitoring tools.

Peripheral Refraction and Aberration Profiles during Accommodation

Many of the peripheral refraction profile characteristics measured in this study were reported previously when using different peripheral refraction techniques. However, because of the required modifications of commercial instruments, measurements were often limited in obtaining certain peripheral eccentricities and/or accommodative demands.

As evidenced in this study, one common characteristic in the distance peripheral refraction profile, which has been linked to myopia development, is that relative to the fovea, myopic eyes are increasingly more hyperopic as visual field angle increases.^{1,6} Another characteristic is the typical nasal-temporal asymmetry

in astigmatism that has been known for many years^{10,36,37} and that can be attributed to the asymmetry of the optical system of the eye.³⁸

More specific to the objectives of the current study, only a few investigations have assessed the effect of accommodation on the peripheral optics of the eye.^{17,26–30} The current study showed that as accommodation increased, the relative peripheral refraction profile (spherical equivalent) shifted from peripheral hyperopia toward peripheral myopia and peripheral against-the-rule astigmatism J_{180} also became increasingly more negative. Peripheral J_{45} was not affected by changes in accommodation. Using a modified Shin-Nippon open-view autorefractor, the study by Whatham et al. measured myopic eyes at horizontal visual field angles of 0, 20, 30, and 40 degrees at distances of 2 m, 40 cm, and 30 cm using head turn. They also showed that as accommodation increased, the relative peripheral refraction profiles of M and J_{180} became significantly more negative, which they attribute to the increasing curvature of the field during accommodation.¹⁷ As shown in the study by Whatham et al., with increasing accommodation, a greater decrease in peripheral J_{180} was found in the nasal visual field when compared with the temporal visual field. However, unlike the study by Whatham et al., this finding was not significant in the present study. Conversely, whereas the current study showed a significant change in the asymmetry of the peripheral refraction profiles of M as a function of accommodation, Whatham et al. did not find such a change.

The study by Calver et al.²⁶ also used the Shin-Nippon open-view autorefractor to measure peripheral refraction along the horizontal visual field meridian at 10, 20, and 30 degrees and at viewing distances of 2.5 m and 40 cm. They concluded that there was no significant correlation between peripheral refraction measurements and viewing distance. Taberero and Schaeffel²⁹ used their new open-view fast-scanning photorefractometer to perform peripheral refraction measurements in 10 emmetropic participants at viewing distances of 200 cm, 50 cm, and 25 cm. They also found no changes in the shape of the peripheral refraction profiles as a function of accommodation. The study by Lundström et al.²⁸ used a modified Hartmann-Shack setup to perform peripheral measurements using eye turn in five emmetropic and five myopic eyes. Measurements were performed at viewing distances of 2 m and 25 cm along the horizontal visual field meridian up to 40 degrees and along the vertical meridian up to 20 degrees. They found that only the peripheral refraction profile of the emmetropic eyes became more myopic with increasing accommodation. With respect to the peripheral higher-order aberrations, they found that there was almost no interaction between accommodative states and peripheral angle, suggesting that the entire aberration profile changes with accommodation. Mathur et al.²⁷ used a modified COAS-HD Hartmann-Shack aberrometer to measure peripheral refractions and higher-order aberrations via eye turn in nine emmetropic participants up to 42 degrees along the horizontal visual field meridian and up to 32 degrees along the vertical visual field meridian at accommodative demands of 0.3 and 4.0 D. When compared with the aberration coefficients assessed in the current study, Mathur et al. found small but significant interactions between accommodative states and peripheral angle for J_{180} , $C[0, 2]$, $C[2, 2]$, $C[2, -2]$, $C[3, 1]$, and $C[3, 3]$. For example, for horizontal coma $C[3, 1]$,

they report a decrease in slope, that is, from -0.006 to -0.005 for measurements performed at 0.3 and 4.0 D, respectively, which is a smaller decrease than found in the current study. Overall, they conclude that based on the results of their relatively small group, the changes in peripheral refraction and higher-order aberrations were only present during accommodation.

Overall, it appears that the changes found in the peripheral refraction and higher-order aberration profiles as a function of accommodation were more substantial in the current study than the changes reported in other studies. This difference can be mainly attributed to the fact that the current study performed measurements over an extended visual field, that is, up to 50 degrees, and for a greater range of accommodative states, that is, up to -5.00 D. Because the greatest relative differences were found at these extended measurement points, the overall results showed a more significant impact of accommodation on the peripheral refraction and higher-order aberration profiles. Other reasons that could have contributed to the differences found between studies could be the use of different peripheral refraction techniques (e.g., instruments; operation principles, i.e., autorefractometry vs. aberrometry; and measurement methods, i.e., eye turn vs. natural viewing conditions), differences in study setup (e.g., sample size, emmetropic/myopic eyes, and age), and the method of analysis (e.g., tilt and curvature coefficients vs. comparison of corresponding visual field points).

Finally, it should be noted that whereas the EM is capable of measuring aberrations along multiple visual field meridians, the aim of the current study was to present the new optical instrument design and its capability of providing peripheral refraction and aberration measurements during accommodation using a fully automated internal fixation target. Further work is in progress to also assess the other visual field meridians.

CONCLUSIONS

The current study showed that significant changes in peripheral refraction and higher-order aberration profiles occurred during accommodation in myopic eyes. With its extended measurement capabilities, that is, permitting rapid peripheral refraction and higher-order aberration measurements up to visual field angles of ± 50 degrees for distance and near (up to -5.00 D), the EM instrument is an advanced instrument that may give additional insights in the ongoing quest to understand and monitor myopia development.

ACKNOWLEDGMENTS

This work was carried out at the clinics and laboratories of the Brien Holden Vision Institute, Sydney, Australia.

Parts of this article have been presented as a poster at the American Academy of Optometry, 2012, Boston. The research was supported in part by the Brien Holden Vision Institute, the Australian Federal Government through the Cooperative Research Centre's Scheme, and the International Postgraduate Research Scholarship (Cathleen Fedtke) through the University of New South Wales, Australia.

The authors extend their thanks to Jiyoung Chung, Pauline Xu, Rebecca Weng, Elise Robertson, Thomas John, and Varghese Thomas for their contributions with data collection and analysis.

Received February 10, 2014; accepted May 15, 2014.

REFERENCES

1. Charman WN, Radhakrishnan H. Peripheral refraction and the development of refractive error: a review. *Ophthalmic Physiol Opt* 2010;30:321–38.
2. Mutti DO, Hayes JR, Mitchell GL, Jones LA, Moeschberger ML, Cotter SA, Kleinstein RN, Manny RE, Twelker JD, Zadnik K. Refractive error, axial length, and relative peripheral refractive error before and after the onset of myopia. *Invest Ophthalmol Vis Sci* 2007;48:2510–9.
3. Smith EL, 3rd, Hung LF, Huang J. Relative peripheral hyperopic defocus alters central refractive development in infant monkeys. *Vision Res* 2009;49:2386–92.
4. Gwiazda JE, Hyman L, Norton TT, Hussein ME, Marsh-Tootle W, Manny R, Wang Y, Everett D. Accommodation and related risk factors associated with myopia progression and their interaction with treatment in COMET children. *Invest Ophthalmol Vis Sci* 2004;45:2143–51.
5. Mutti DO, Mitchell GL, Hayes JR, Jones LA, Moeschberger ML, Cotter SA, Kleinstein RN, Manny RE, Twelker JD, Zadnik K. Accommodative lag before and after the onset of myopia. *Invest Ophthalmol Vis Sci* 2006;47:837–46.
6. Fedtke C, Ehrmann K, Holden BA. A review of peripheral refraction techniques. *Optom Vis Sci* 2009;86:429–46.
7. Ferree CE, Rand G, Hardy C. Refraction for the peripheral field of vision. *Arch Ophthalmol* 1931;5:717–31.
8. Ronchi L. Absolute threshold before and after correction of oblique-ray astigmatism. *J Opt Soc Am* 1971;61:1705–9.
9. Wang YZ, Thibos LN, Lopez N, Salmon T, Bradley A. Subjective refraction of the peripheral field using contrast detection acuity. *J Am Optom Assoc* 1996;67:584–9.
10. Rempt F, Hoogerheide J, Hoogenboom WP. Peripheral retinoscopy and the skiagram. *Ophthalmologica* 1971;162:1–10.
11. Johnson CA, Leibowitz HW. Practice, refractive error, and feedback as factors influencing peripheral motion thresholds. *Percept Psychophys* 1974;15:276–80.
12. Jennings JA, Charman WN. Optical image quality in the peripheral retina. *Am J Optom Physiol Opt* 1978;55:582–90.
13. Navarro R, Moreno E, Dorronsoro C. Monochromatic aberrations and point-spread functions of the human eye across the visual field. *J Opt Soc Am (A)* 1998;15:2522–9.
14. Seidemann A, Schaeffel F, Guirao A, López-Gil N, Artal P. Peripheral refractive errors in myopic, emmetropic, and hyperopic young subjects. *J Opt Soc Am (A)* 2002;19:2363–73.
15. Lundström L, Gustafsson J, Unsbo P. Vision evaluation of eccentric refractive correction. *Optom Vis Sci* 2007;84:1046–52.
16. Atchison DA, Pritchard N, White SD, Griffiths AM. Influence of age on peripheral refraction. *Vision Res* 2005;45:715–20.
17. Whatham A, Zimmermann F, Martinez A, Delgado S, de la Jara PL, Sankaridurg P, Ho A. Influence of accommodation on off-axis refractive errors in myopic eyes. *J Vis* 2009;9:141–3.
18. Atchison DA, Scott DH, Charman WN. Measuring ocular aberrations in the peripheral visual field using Hartmann-Shack aberrometry. *J Opt Soc Am (A)* 2007;24:2963–73.
19. Mathur A, Atchison DA, Scott DH. Ocular aberrations in the peripheral visual field. *Opt Lett* 2008;33:863–5.
20. Mathur A, Atchison DA. Peripheral refraction patterns out to large field angles. *Optom Vis Sci* 2013;90:140–7.
21. Fedtke C, Ehrmann K, Ho A, Holden BA. Lateral pupil alignment tolerance in peripheral refractometry. *Optom Vis Sci* 2011;88:570–9.
22. Taberero J, Schaeffel F. More irregular eye shape in low myopia than in emmetropia. *Invest Ophthalmol Vis Sci* 2009;50:4516–22.
23. Jaeken B, Artal P. Fast Hartmann-Shack wavefront sensor for the periphery. *Invest Ophthalmol Vis Sci* 2010;51:E-abstract 4303.
24. Wei X, Thibos L. Design and validation of a scanning Shack Hartmann aberrometer for measurements of the eye over a wide field of view. *Opt Express* 2010;18:1134–43.
25. Fedtke C, Ehrmann K, Falk D, Holden B. Validation of a quasi real-time global aberrometer: the EyeMapper. In: Manns F, Söderberg PG, Ho A, eds. *Proceedings of SPIE Ophthalmic Technologies XXII Meeting*, San Francisco, California, January 21, 2012. Available at: <http://dx.doi.org/10.1117/12.906927>. Accessed July 1, 2014.
26. Calver R, Radhakrishnan H, Osuobeni E, O'Leary D. Peripheral refraction for distance and near vision in emmetropes and myopes. *Ophthalmic Physiol Opt* 2007;27:584–93.
27. Mathur A, Atchison DA, Charman WN. Effect of accommodation on peripheral ocular aberrations. *J Vis* 2009;9:201–11.
28. Lundström L, Mira-Agudelo A, Artal P. Peripheral optical errors and their change with accommodation differ between emmetropic and myopic eyes. *J Vis* 2009;9:17.1–11.
29. Taberero J, Schaeffel F. Fast scanning photoretinoscope for measuring peripheral refraction as a function of accommodation. *J Opt Soc Am (A)* 2009;26:2206–10.
30. Smith G, Millodot M, McBrien N. The effect of accommodation on oblique astigmatism and field curvature of the human eye. *Clin Exp Optom* 1988;71:119–25.
31. Delori FC, Webb RH, Sliney DH. Maximum permissible exposures for ocular safety (ANSI 2000), with emphasis on ophthalmic devices. *J Opt Soc Am (A)* 2007;24:1250–65.
32. Bakaraju RC, Fedtke C, Ehrmann K, Falk D, Weng R, Sankaridurg P, John T, Ho A, Holden B. Validation of accommodative responses measured with the EyeMapper. *Invest Ophthalmol Vis Sci* 2012;53:E-abstract 1354.
33. Wagner S, Conrad F, Bakaraju RC, Fedtke C, Ehrmann K. Power profiles of single vision soft contact lenses. *Cont Lens Anterior Eye* 2013;36:e33.
34. Radhakrishnan H, Charman WN. Peripheral refraction measurement: does it matter if one turns the eye or the head? *Ophthalmic Physiol Opt* 2008;28:73–82.
35. Mazzaferri J, Navarro R. Wide two-dimensional field laser ray-tracing aberrometer. *J Vis* 2012;12.
36. Ferree CE, Rand G, Hardy C. Refractive asymmetry in the temporal and nasal halves of the visual field. *Am J Ophthalmol* 1932;15:513–22.
37. Millodot M. Effect of ametropia on peripheral refraction. *Am J Optom Physiol Opt* 1981;58:691–5.
38. Dunne MC, Misson GP, White EK, Barnes DA. Peripheral astigmatic asymmetry and angle alpha. *Ophthalmic Physiol Opt* 1993;13:303–5.

Cathleen Fedtke

Brien Holden Vision Institute

Level 4, North Wing

Rupert Myers Bldg, Gate 14

Barker St, The University of New South Wales

Sydney, New South Wales 2052

Australia

e-mail: c.fedtke@brienholdenvision.org